

Document downloaded from:

<http://hdl.handle.net/10251/194944>

This paper must be cited as:

García Martínez, A.; Monsalve-Serrano, J.; Martínez-Boggio, SD.; Zhao Wenbin; Qian, Y. (2022). Intelligent charge compression ignition combustion for range extender medium duty applications. *Renewable Energy*. 187:671-687. <https://doi.org/10.1016/j.renene.2022.01.110>



The final publication is available at

<https://doi.org/10.1016/j.renene.2022.01.110>

Copyright Elsevier

Additional Information

Intelligent charge compression ignition combustion for range extender Medium Duty Applications

Antonio García^a, Javier Monsalve-Serrano^{*a}, Santiago Martinez-Boggio^a, Wenbin Zhao^b, Yong Qian^b

Renewable Energy

Volume 187, March 2022, Pages 671-687

<https://doi.org/10.1016/j.renene.2022.01.110>

^aCMT - Motores Térmicos, Universitat Politècnica de València, Camino de Vera s/n, 46022 Valencia, Spain

^bKey Laboratory for Power Machinery of M.O.E, Shanghai Jiao Tong University, Shanghai 200240, China

Corresponding author (*):

Dr. Javier Monsalve-Serrano (jamonse1@mot.upv.es)

Phone: +34 963876559

Fax: +34 963876559

Abstract

Electrified powertrains have been growth in the last few years due to the increase in powertrain efficiency. However, for heavy-duty vehicles the right choice it is not clear. The long-routes and large number of daily kilometres makes that current battery technology it is not prepared to cover the minimum requirements. A mid-term solution is hybrid powertrains. The mix between pure electric range and range extender mode in liquid fuels make perfect to complete a large distance. However, tailpipe pollutant and CO₂ emissions are still a disadvantage against pure electric powertrain. This study analyses the potential of hybrid powertrains running in an advanced combustion mode as Intelligent Charge Compression Ignition. Due to the flexibility of the combustion mode different renewable energy fuels are tested: Butanol, Methanol and Biodiesel. The work is focused in urban buses due to the potential of electrified powertrains in this context and the large number of vehicles concentrated in cities. The results show that pure electric bus reduce 54% the CO₂ emissions at LCA level. Meanwhile the Intelligent Charge Compression Ignition allows to 32% with one renewable fuel (Diesel-Butanol) and 66% with two renewable fuels (Biodiesel-Methanol) with respect to the non-hybrid diesel reference.

Keywords

Renewable Energy; Advanced Combustion Mode; Electrified Powertrain; Life Cycle Analysis

41 1. Introduction

42 Heavy-duty vehicles including buses, delivery and other utility trucks, are the new
43 focus of research because are usually operated based on defined daily routes and have
44 large emissions due to the total weight [1]. Therefore, a number of cities are already
45 paying attention on cleaner public transport, while many bus operators are renewing
46 their fleet or deploying low-emission vehicles. Options as Battery Electric Vehicles (BEV),
47 Plug-In Hybrid Electric Vehicles (PHEV), Full Hybrid Electric Vehicles (FHEV) and Mild
48 Hybrid Electric Vehicles (MHEV) are appear in the recent years [2].

49 Inside hybrid vehicles exist a large offer of powertrain architectures. Hybrid urban
50 buses are considered as one such option, with the main reduction in costs expected from
51 a decreased fuel consumption (FC) over conventional buses. Powertrain simulation
52 results indicate that both parallel and series hybrid systems can offer fuel economy
53 benefits up to 45% over conventional buses [3][4]. Results from experimental
54 assessments vary. Gerbec et al. [5] found that the FC of a hybrid-diesel bus was 15–18%
55 lower than a corresponding conventional one, depending on traffic conditions in the city
56 of Poznan, Poland. Hallmark et al. [6] reported an average 11.8% higher fuel economy
57 of three hybrid buses than two conventional ones in Iowa, USA. Hu et al. [7] observed a
58 30% fuel savings potential, after examining the results of one hybrid bus over a
59 conventional one in Sakarya, Turkey. Guo et al. [8] also reported significant fuel benefits
60 from two parallel hybrid buses over conventional ones, but the variability in driving
61 conditions did not make possible to precisely quantify the improvement. Zhang et al. [9]
62 analysed on-road emissions of 75 Euro II to Euro V transit buses in Beijing, China,
63 including two Euro IV single deck hybrid-diesel buses. Hybrid-diesel buses were found
64 to consume 29% less fuel compared to conventional ones. Moreover, Range Extender
65 Vehicles (REV) use an onboard electricity generator to provide additional energy if the
66 battery is depleted during operation [10]. This allows to reduce the battery pack size
67 compared to BEV. REV can be PHEV or FHEV depends if is added an external connection
68 for grid charging during parking. However, the optimal component selection when is
69 combined elements of conventional powertrain and BEV is not trivial. In addition, the
70 control system of this components increases in complexity. The right selection is crucial
71 to find the optimal trade-off between fuel economy, drivability, and vehicle cost [11].
72 Therefore, multiple performance objectives are the best option [12]. Depends on the
73 vehicle use segment, public transports or trucks for parcel delivery, the same powertrain
74 may not be optimal in all situations [13]. Therefore, is extensively used the numerical
75 evaluation for vehicle evaluation for powertrain sizing under driving scenarios
76 representing realistic driving missions [14]. Compared to parallel and power-split hybrid
77 vehicle architectures, which have less battery capacity, REVs reduce the transient
78 behaviour of the internal combustion engine (ICE) because the wheels are uncoupled
79 for the ICE and electric machine (EM) generator. This allows to operate the engine along
80 the optimal operation line at desired rotational speed [10]. This make a new scenario
81 for the application of advanced combustion modes [15].

82 Several technologies are available for emissions control in diesel engines. The
83 current emissions control systems used to meet the European Union (EU VI) limits rely
84 in passive actions as selective catalytic reduction (SCR) for NO_x emissions control. To
85 comply with the 10-ppm ammonia limit, averaged over the World Harmonized Transient
86 Cycle, ammonia slip catalysts (ASC) are widely used. For particle control, diesel
87 particulate filters (DPF) are present in all EU VI compliant systems, heavily relying on a
88 diesel oxidization catalyst (DOC) for passive and active regeneration [16]. This means a
89 large and expensive aftertreatment system to mitigate the emissions generated in the
90 combustion chamber. In the EU VI normative this is enough but beyond 2025 is expected
91 to be introduced EU VII [17]. This new restriction will have 90% lower NO_x than EU VI
92 [18]. Also, modification of the on-road test used in type-approval, in-service conformity,
93 and market surveillance is expected, with an emphasis on shorter trips, low-load, and
94 cold-start operation. Similar to Europe, China is in the preparatory groundwork to
95 develop China VII standards to be applied beyond 2025. Therefore, reducing engine-out
96 emissions is crucial nowadays. Low temperature combustion modes as homogeneous
97 controlled compression ignition (HCCI) [19] and premixed charged compression ignition
98 (PCCI) [20] have been studied in the last years. Low emissions and high efficiency were
99 expected to be simultaneously achieved if combustion takes place under homogeneous
100 or slightly stratified conditions in advanced combustion modes. Main barriers that
101 obstruct these modes is the absent of direct methods to control the ignition timing
102 (mainly in HCCI). Therefore, it is seen high-pressure rising rate under higher engine load
103 and misfire under lower engine load (mainly in PCCI). To overcome this issue, some
104 researches has proposed the Reactivity Controlled Compression Ignition (RCCI)
105 combustion mode [21] that enables a higher control of the combustion process by the
106 use of two fuels with different reactivity. This allows to create a mixture stratification
107 among the temperature stratification seen in HCCI. The high reactivity fuel (Diesel,
108 dimethyl ether DME, oxymethylene dimethyl ethers OMEx) is injected directly in the
109 combustion chamber (DI) and the low reactivity fuel (Gasoline, Ethanol, Methanol) in
110 the port fuel injector (PFI). This combustion concept is applied in Compression Ignition
111 (CI) engines. The main advantage is that combines elements seen in conventional
112 combustion modes commercially available (CI Diesel and Spark Ignited (SI) Gasoline).
113 The main drawback is that the port injection might cause rich fuel areas and fuels being
114 trapped in crevice regions. This increase HC and CO emissions even higher than SI mode
115 because of the large crevices of CI engines. To improve even more the combustion
116 concept a new dual-fuel combustion mode appears in the recent years called: Intelligent
117 Charge Compression Ignition (ICCI) combustion mode [22]. The main advantage is the
118 flexibility to inject the Low Reactivity Fuel (LRF) in both DI and PFI. This allows a better
119 stratification by selecting the best reactivity gradient according to engine operating
120 condition. In the ICCI mode, most of low-reactivity fuel is directly injected during the
121 intake stroke with single or multiple stage split injection [23]. Then, the rest of low-
122 reactivity fuel and high-reactivity fuel are directly injected in succession to establish
123 crossed stratifications of the equivalence ratio and reactivity in the cylinder. Under the
124 various engine loads, ICCI mode can form flexible stratifications to control the heat

125 release by adjusting injection parameters such as injection timings, stages of split
126 injection, and energy ratios of fuels, etc [24].

127 In this work, the powertrain design of an urban bus is considered. The bus has a
128 series hybrid powertrain with an internal combustion engine as range extender where
129 the correct sizing and emissions reduction potential are explored. The powertrain is
130 optimized for different driving cycles to analyse how the driving mission and passengers
131 affects the selected powertrain. A simulation model of the powertrain is developed and
132 optimization strategies are used to compute the optimal battery and engine sizing.
133 Later, a novelty combustion concept is tested with conventional and renewable energy
134 fuels as Bio-Diesel, Methanol and Butanol. The dual-fuel concept shows great potential
135 to mitigate the high-volume consumption of these low heating value fuels. In addition,
136 the stratified temperature and reactivity help to strongly reduce the engine-out
137 emissions. The results are compared against conventional powertrains and pure electric
138 bus in an life cycle analysis (LCA) basis. Therefore, the main novelty of this work is a new
139 methodology to optimize hybrid range extender buses based in real driving cycles. In
140 addition, this work presents results for a standard bus in different powertrain
141 technologies analysed in European and Asia context. Emissions as CO₂ in different basis
142 as well as NO_x, HC and CO are presented for different fuels. This add interesting
143 information that can not be found in the bibliography up to the knowledge of the
144 authors.

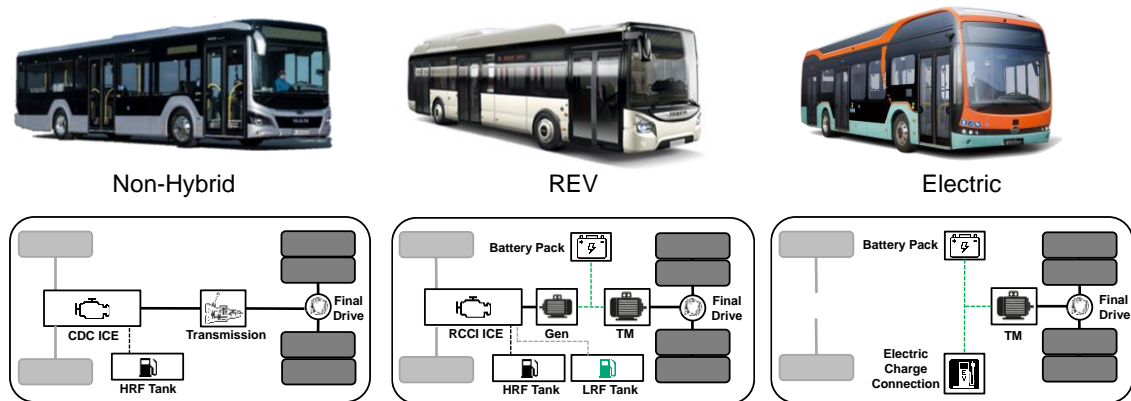
145 **2. Methodology**

146 In this section is presented the methodology used for the study of ICCI combustion
147 mode in a REV. The bus vehicle model, driving cycles used to test the concept under
148 transient conditions, powertrain design, combustion experimental data and life cycle
149 analysis approach is presented.

150 **2.1. Vehicle Model**

151 Three powertrains are studied in this work, including a non-hybrid powertrain
152 operating with diesel (representative of the most used current system in the market
153 [25]), REV operating under a low temperature combustion mode with two fuels and a
154 pure battery electric bus (representative of zero tailpipe emissions vehicle available in
155 the market [26]). The work will be focus in optimize the REV and compare with the
156 baseline non-hybrid and pure electric buses. The base of the REV truck is based in a
157 IVECO Urbanway series hybrid [27]. Figure 1 show the vehicles used and a scheme of the
158 components layout that are simulated in the OD vehicle model. The vehicles are model
159 in GT-Suite V2021 (Gamma Technologies) and the main components specification for
160 the baseline cases (Non-hybrid and Electric) are taken from manufacturer publications.
161 The powertrain validation was done by the authors in previous manuscript with a Volvo
162 FL 18-tons medium duty truck [28]. This vehicle has the same engine and powertrain
163 components that the Volvo 7900 (equivalent to the MAN Lion City). The results show a
164 difference below 2% in fuel consumption with a good agreement in terms of power and
165 torque prediction. The REV is designed in current work to efficiently work under ICCI

166 combustion mode. Therefore, ICE and battery size are optimized by a Design of
 167 Experiments (DoE).



168
 169
 170
 171

Figure 1 – Bus Models used to evaluate a conventional powertrain (non-hybrid CI Diesel), range extender vehicle (REV with dual fuel ICCE concept) and pure electric bus BEV). The model are created using GT-Suite 2021 from Gamma Technologies®.

172 Table 1 shows the main bus specifications. The battery pack is simulated by a stack
 173 of series and parallel cylindrical cells (3.3 V and 2.5 Ah from A123 Lithium-Ion phosphate
 174 LFP [29]). The electric machine is model by JMAG software using the rated power and
 175 torque specifications [30]. The efficiency map obtained is introduced in the GT-SUITE
 176 electric machine model. Transmission components are simulated with average
 177 efficiency of 0.97. Lastly, the ICE is simulated with experimental engine test bed
 178 stationary maps. This method allows to an accurate and fast simulation of the fuel
 179 consumption and engine-out emissions.

180

Table 1. Bus specifications by type: Non-Hybrid, REV and Electric.

Parameter	Non-Hybrid	REV	Electric
Model Name	MAN Lion's City	Prototype	BYD 12m eBus
Engine Type	Diesel, EUVI compliant with ATS, CI engine	Dual-Fuel ICCE, CI engine	-
Maximum Passenger Capacity	70		
Gross Weight (Kg)	19000	19500	20000
Rated Power - Engine/Motor (kW)	265 / -	To be designed	- /150 x 2
Maximum Torque – Engine/Motor (Nm)	1600 /	To be designed	/ 550x2
Battery Capacity (kWh)	-	To be designed	348
Length (mm)	12000		
Width (mm)	2550		
Height (mm)	3060	3280	3370

181

182

2.2. Bus Routes

183

184

185

186

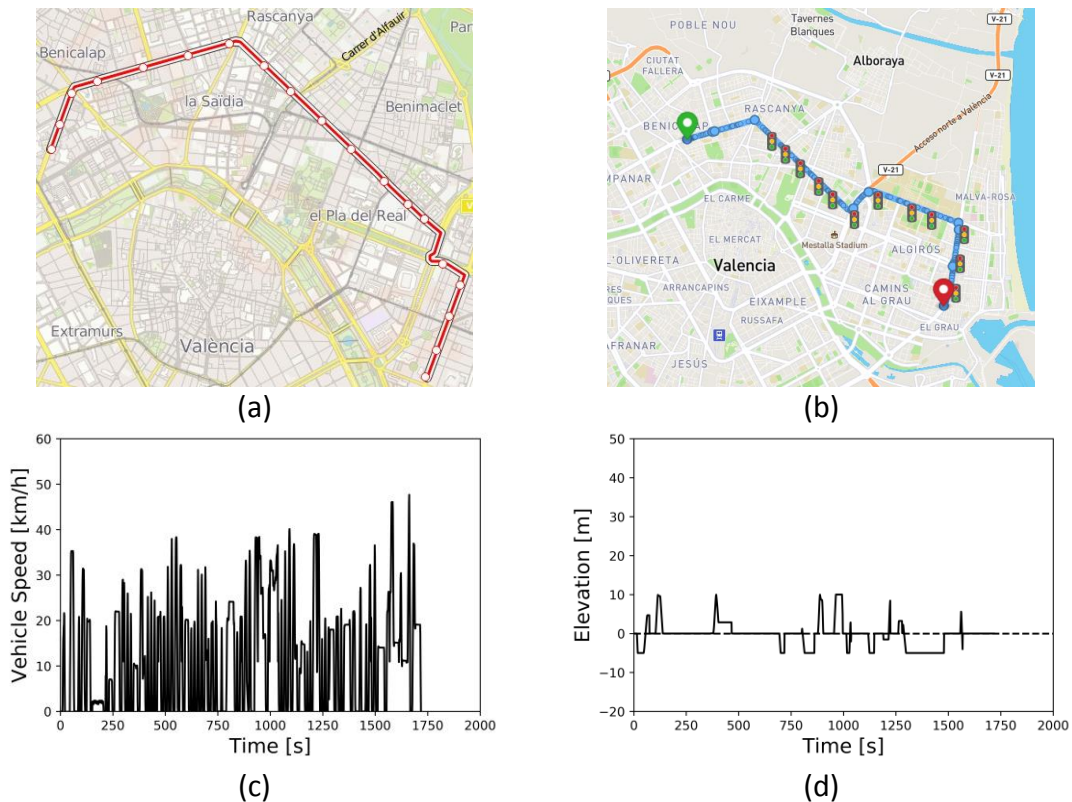
187

188

189

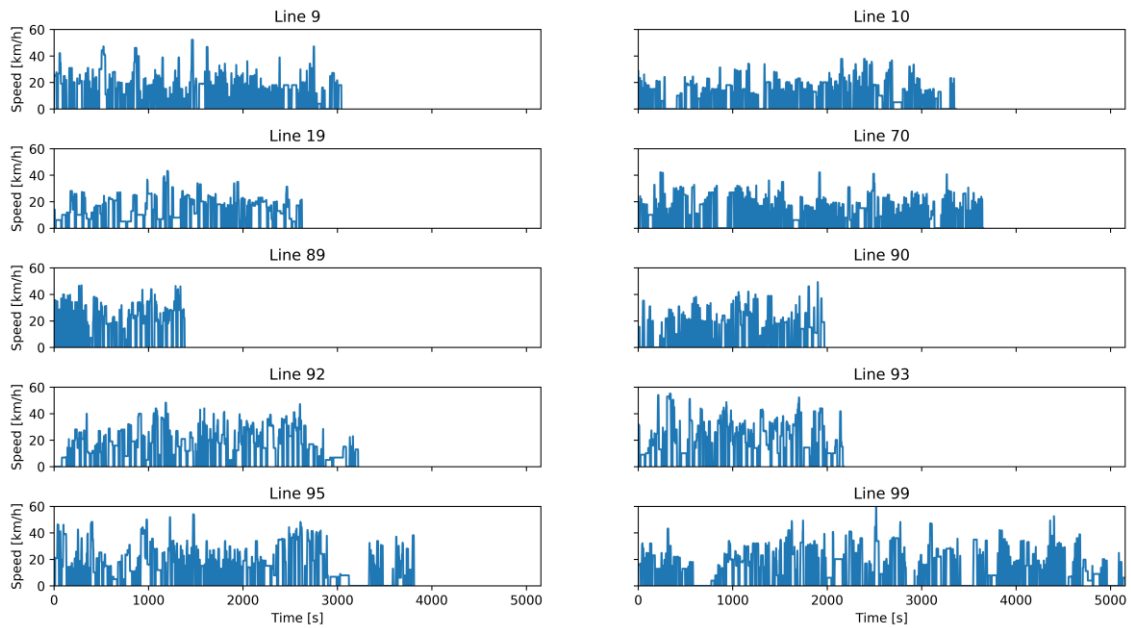
The vehicles are simulated in transient conditions representatives of real routes in two different scenarios. It was selected Europe (Valencia, Spain) and Asia (Shanghai, China) due to the different vehicle use (city population, geography and traffic) and electric mix (Europe based in Renewable energy 38% and Fossil 35% [31] meanwhile China mainly Fossil 65% and Renewable energy 27% [32]). This will allow to compare the non-hybrid, REV and Electric performance and total emissions in two drastically different scenarios. To obtain the routes, an online driving cycle generator is used called GT-

190 RealDrive. This plugin of GT-SUITE allows in real time using MapBox tools [33] to obtain
 191 the vehicle speed and elevation profile against the distance travelled. After simulate the
 192 route with the OD vehicle model is possible to obtain the real speed profile against time
 193 depends on the vehicle performance. This will guarantee a correct vehicle sizing testing
 194 environment. Figure 2 shows the driving cycle methodology scheme in an example case
 195 of one-line bus in Valencia, Spain. First the route is taken from the city bus company
 196 with the trajectory and stops. Later, the start and end of the route is inserted in GT-
 197 RealDrive with the via points marked as the stops. In each stop, the vehicle stays 30
 198 seconds, representative of an average bus stop. The speed profile and altitude are
 199 obtained against time. It is important that traffic level and signals are considering in the
 200 route generation.



201 Figure 2 – Driving cycles method. Example bus line 90 in Valencia, Spain. Line stop obtained from
 202 EMT Valencia (a). The bus line is built in GT-RealDrive 2021 from Gamma Technologies® (b). The vehicle
 203 speed (c) and elevation (d) along the time is obtained after run the simulation.

204 Figure 3 and Figure 4 shows ten driving cycles representative of the most used routes
 205 in Valencia and Shanghai, respectively. It is possible to see that the total time that a bus
 206 needs to complete the route goes between 30 minutes to 85 minutes. The maximum
 207 speed not exceed the 60 km/h in any case with some flat vehicle phases representative
 208 of traffic jams.

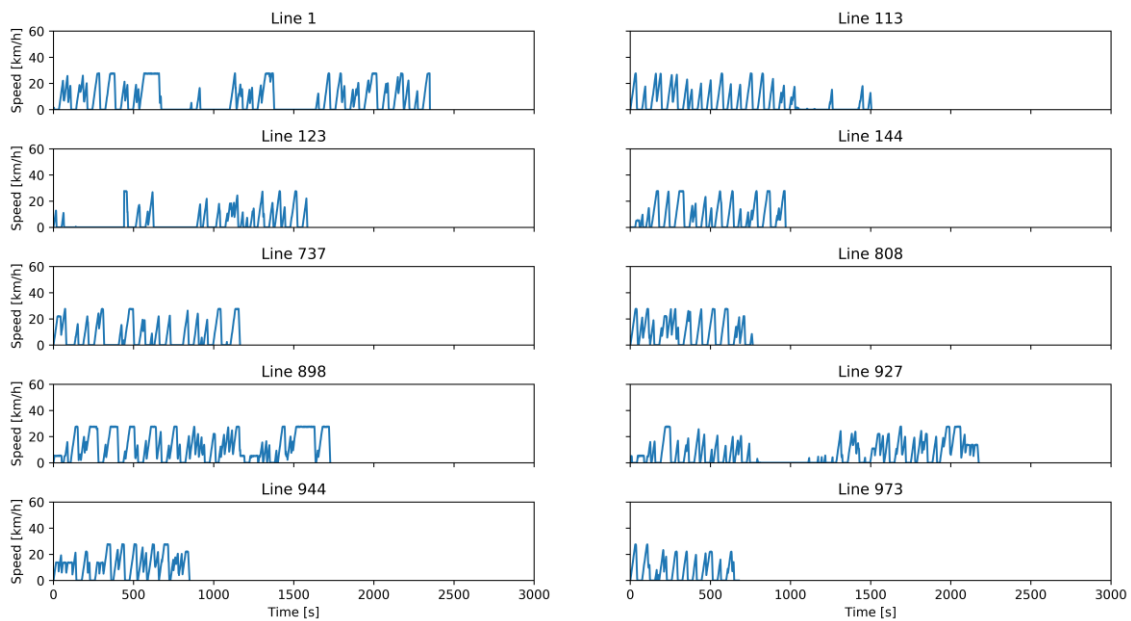


209

210

211

Figure 3 – Ten main bus lines in Valencia: 9, 10, 19, 70, 89, 90, 92, 93, 95, 99. The driving cycles are representative of Europe conditions and used to evaluate the different buses configurations.



212

213

214

215

Figure 4 – Ten main bus lines in Shanghai: 1, 113, 123, 144, 737, 808, 898, 927, 944 and 973. The driving cycles are representative of Asia conditions and used to evaluate the different buses configurations.

216

217

218

219

For the vehicle simulations, the mass of a passenger was defined as 68 kg. This is used in the Federal Transit Administration (FTA) bus testing regulations [34]. Several cases will be tested ranging from empty bus up to 70 passenger (max passenger capacity) that represents 4760 kg.

220

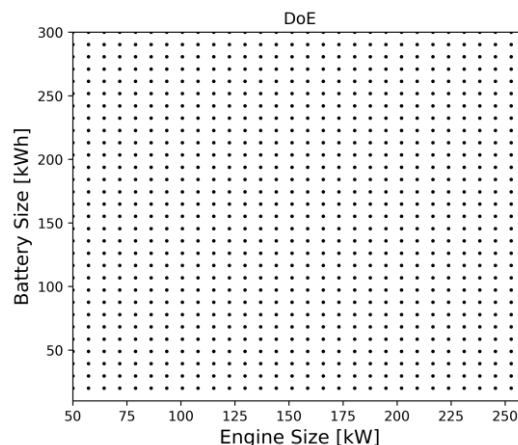
2.3. Optimization and Performance Procedure

221

222

To correctly size the REV, the battery and internal combustion engine energy capacity and power are studies, respectively. An optimization with a DoE of 400 cases is

223 used with a range between 20 (minimum to feed the EM) to 300 kWh (representative of
 224 a pure electric bus) for the battery and 50 to 280 kW of engine size (see Figure 5). The
 225 battery is scaled by a Thevenin equivalent cell model, adding cells in parallel
 226 configuration. The battery pack is maintained in 600V representative of current vehicles
 227 in the market. In the case of the ICE, it is supposed a fixed brake thermal efficiency (BTE)
 228 of 40% for this first optimization approach. As the ICE operates in a generator mode with
 229 a specific operating condition this assumption is conservative. For a conventional diesel
 230 combustion, the maximum BTE can achieve 43% and above BTE of 40% in medium to
 231 high engine load [26]. For advanced combustion modes the values can be even higher,
 232 as will be demonstrated later in the manuscript. Despite is a strong hypothesis, it is
 233 useful to size the engine and battery with a simple DoE approach. The assumption
 234 cannot be done if the operating condition is three time lower than the maximum engine
 235 size. Summarizing, for a selected driving cycle a DoE is run to obtain the final fuel
 236 consumption. The total vehicle fuel consumption for different battery size and engine
 237 power is obtained. The minimum fuel consumption case is taken as optimum. Therefore,
 238 for this section of the work is supposed to work with pure diesel with a BTE of 40%.
 239 Later, the ICCI with different fuel will be evaluated. Figure 5 shows the DoE test matrix.
 240 Full factorial with 20 levels is used to a deep space search.



241

Figure 5 – DoE space search for battery and internal combustion engine sizing.

242

243

244

245

246

247

248

249

250

251

252

253

254

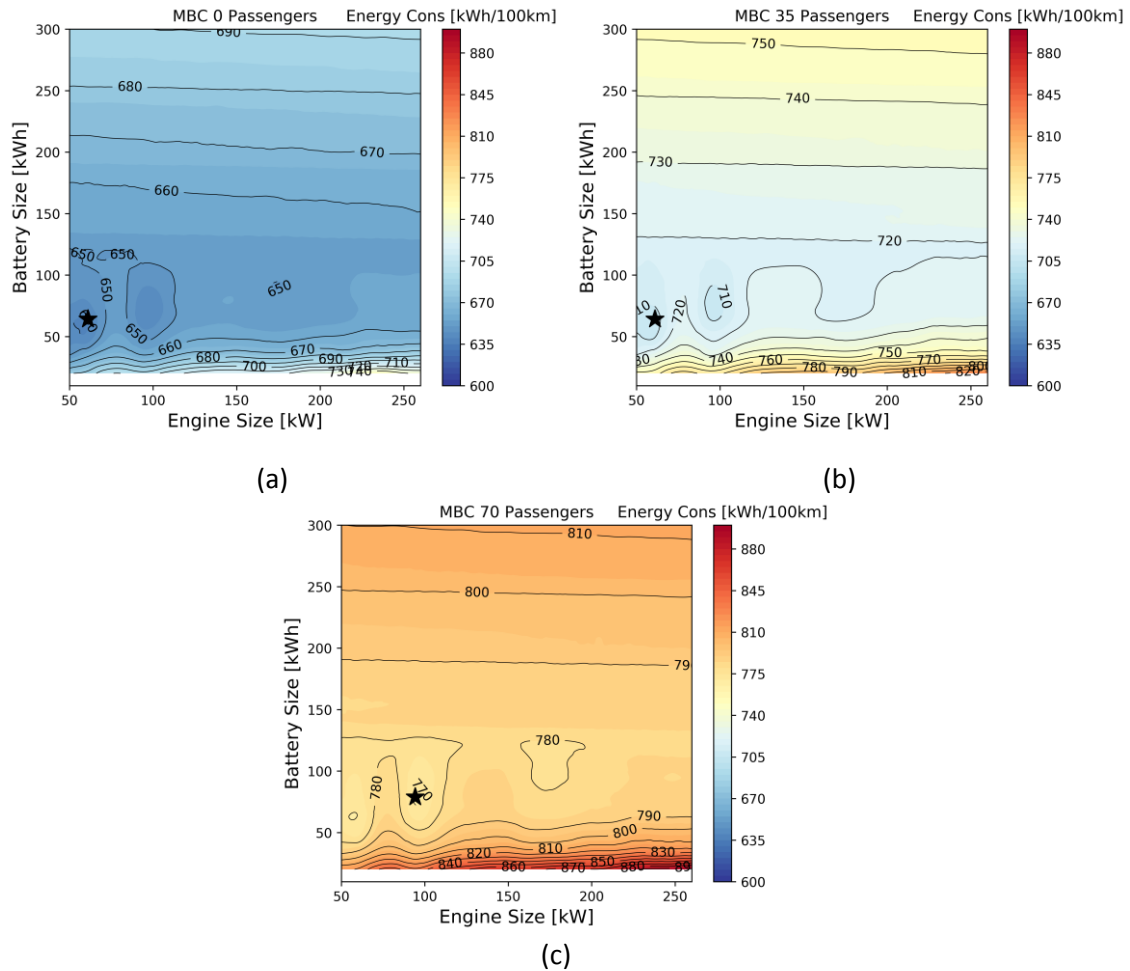
255

256

To preliminary evaluate the bus in a well-known driving cycle, Manhattan Bus
 Cycle (MBC) is used [35]. The Manhattan cycle was developed based on actual
 observed driving patterns of urban transit buses in the Manhattan core of New York
 City. The cycle is characterized by frequent stops and very low speed. Later in the
 manuscript Valencia and Shanghai cycle will be used. This MBC cycle is useful for
 bibliography comparison of the results.

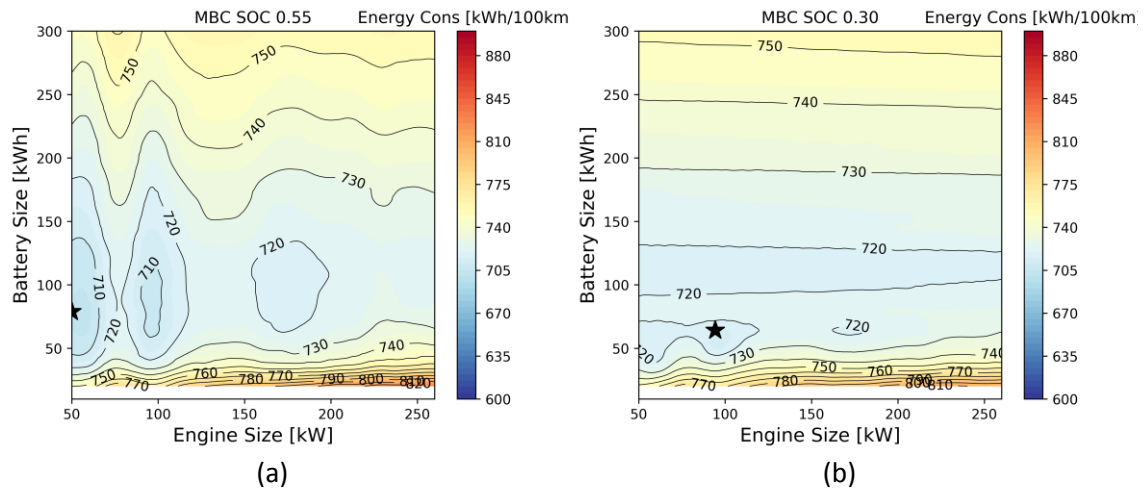
Figure 6 shows the DoE results for MBC driving cycle with different passenger
 load. It was tested from 0, 35 and 70 passengers. For empty and medium load cases
 the optimum is found at 60 kW of ICE power and 64 kWh of battery size. The full bus
 case increases to 94 kW of ICE power and 79 kWh energy capacity. In spite of the
 change in ICE power, low battery size (< 50 kWh) increases the fuel consumption.
 The isolines of fuel consumption are almost linear for different ICE power for a
 battery size. Therefore, the battery size is seen as a more critical parameter. In

257 addition, from Figure 6 it is possible to understand the passenger effect between
 258 empty bus to full bus. The fuel consumption increases 20% in the optimum case. If
 259 compare the optimum case for empty truck (same as 35 passenger, 60 kW ICE and
 260 64 kWh battery) at 70 passenger loads, the case increases 1% with respect to the
 261 optimum (94 kW ICE and 79 kWh battery). Therefore, as the idea is to reduce sources
 262 the lower component size is the best selection in this case.



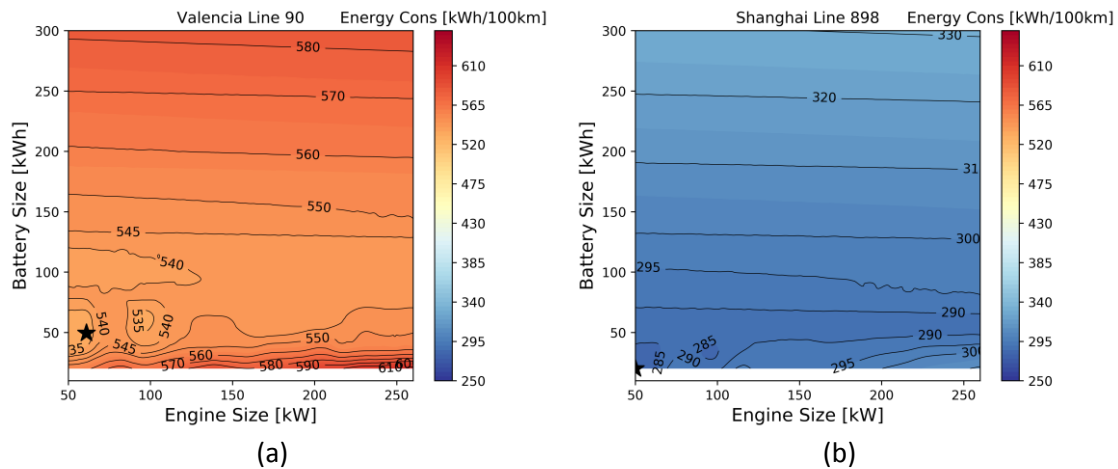
263 Figure 6 – Bus passenger influence with 0 (a), 35 (b) and 70 (c) with a SOC to charge of 0.45 in the
 264 Manhattan Bus Cycle.

265 Figure 7 shows the DoE results for MBC driving cycle at different battery
 266 management strategy. The battery value evaluated is the state of charge (SOC) at
 267 which the battery changes from pure electric mode to battery charge mode (the ICE
 268 is turn on to return the energy to the battery up to the initial level 0.6). Three SOC
 269 charge values are analysed at: 0.55 (Figure 7a), 0.45 (Figure 6b) and 0.30 (Figure 7b).
 270 The last value is selected close to the minimum recommendable of 0.25 for the type
 271 of cell used in the current study. The results show that for the optimum selection it
 272 has a low influence in the results with the optimum at 0.55. The 0.45 and 0.30 gives
 273 an increase of 0.5% and 1.5% at the optimum. It is remarkable from the results that
 274 0.55 gives worst values at high battery capacity due to the excess of weight in the
 275 bus and the no use of the battery energy due to the narrow range of the operative
 276 SOC.



277 Figure 7 – Bus SOC influence at 0.55 (a), and 0.30 (b) with a passenger load of 35 in the Manhattan Bus
 278 Cycle .

279 Figure 8Figure 7 shows the DoE results for driving cycles in Valencia and Shanghai.
 280 Also, this result can be compared with Figure 6b. It possible to see that the cycle has
 281 a strong impact in the final fuel consumption results. Valencia cycle has 24% of less
 282 fuel consumption. Mainly this depends on the regenerating braking and the amount
 283 of start of stops of the cycle. On the other hand, for the same passenger load the
 284 optimum for the ICE and battery size are the same. This is a strong point of the
 285 powertrain due to the flexibility to apply in different cycles.



286 Figure 8 – Bus in the Valencia line 90 (a) and Shanghai line 898 (b) with a passenger load of 35 and SOC
 287 of 0.45.

288 Figure 9Figure 7 shows the DoE results for MBC cycle but at different driving
 289 length. One MBC takes 1089 s (18.2 min), so the cycle was repeated up to complete
 290 1, 5 and 15 hours. The results can be compared with Figure 6b. The fuel consumption
 291 is close between cycles. The unique differences are at high battery size were the
 292 pure electric mode has larger effect when increase the driving distance. However, as
 293 the battery need to be recharged by the ICE the efficiency of the powertrain not has
 294 large improvements. It is important to note that the cases with high duration implies
 295 high computational cost. Therefore, from this analysis can be obtained that one MBC
 296 is enough to have an accuracy fuel consumption value for a daily bus operation.

297

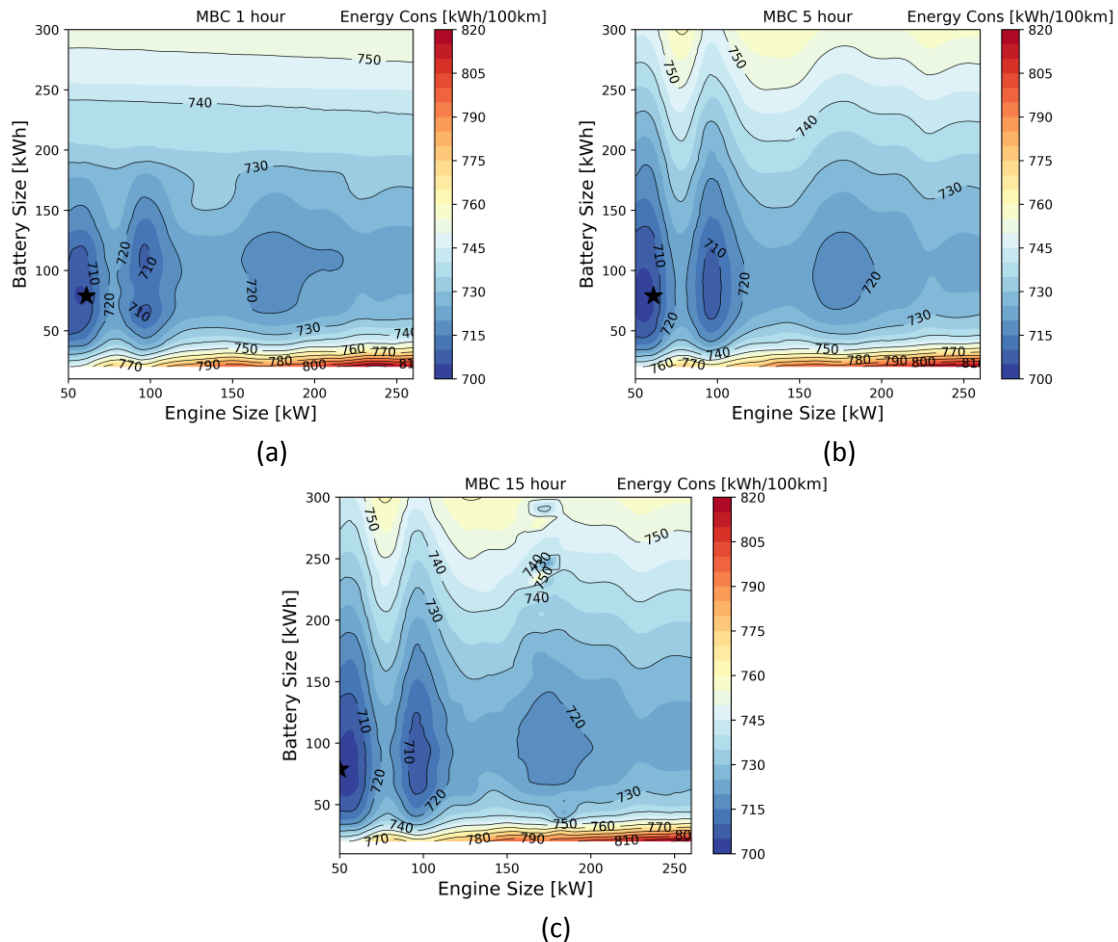


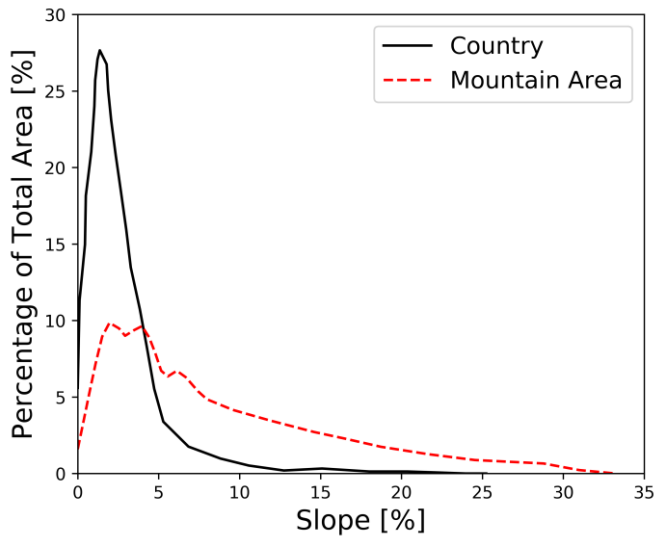
Figure 9 – Bus operational time 1 hour (a), 5 hours (b), and 15 hours (c).

298

299 In spite of the DoE optimization for a particular daily driving cycle, the OEM and
 300 costumers want that the bus can operate also in extreme conditions. To analyse this,
 301 a performance vehicle analysis is the right tools. By a MATLAB vehicle model code,
 302 the maximum wheel force depends on the REV mode is shown in Figure 10. For
 303 comparison the six gear non-hybrid bus is plotted. The EV mode of the REV represent
 304 the condition of a battery enough charged to deliver all the required power to feed
 305 the EM. On the other hand, the hybrid charge sustaining (HEV CS) represents the
 306 condition of the battery depleted and the ICE delivering the required power. Three
 307 different conditions are tested representing an ICE maximum power of: 50 kW, 100
 308 kW and 150 kW. It is possible to see that in EV mode the wheel force is higher than
 309 Non-hybrid bus until 15 km/h. Above 20 km/h the non-hybrid has large power due
 310 to a more powerful ICE than the REV TM. In spite of the lower wheel force, both
 311 vehicles achieve 120 km/h and allows uphill higher than 20% grade with vehicle
 312 speed at least of 25 km/h. It is important to note that this study is performed with
 313 the bus totally loaded. When the ICE in the REV is turn on and the battery is totally
 314 depleted the REV maximum wheel force decrease. With 50 kW of ICE the bus cannot
 315 perform uphill higher than 15% and uphill of 5% only up to 20 km/h. When increase
 316 to 100 kW the capabilities increase up to 30% and 40 km/h, respectively. Lastly, the
 317 150 kW achieves 45% and 55 km/h. Analysing the road inclination of different

318

geographies, it is possible to see in



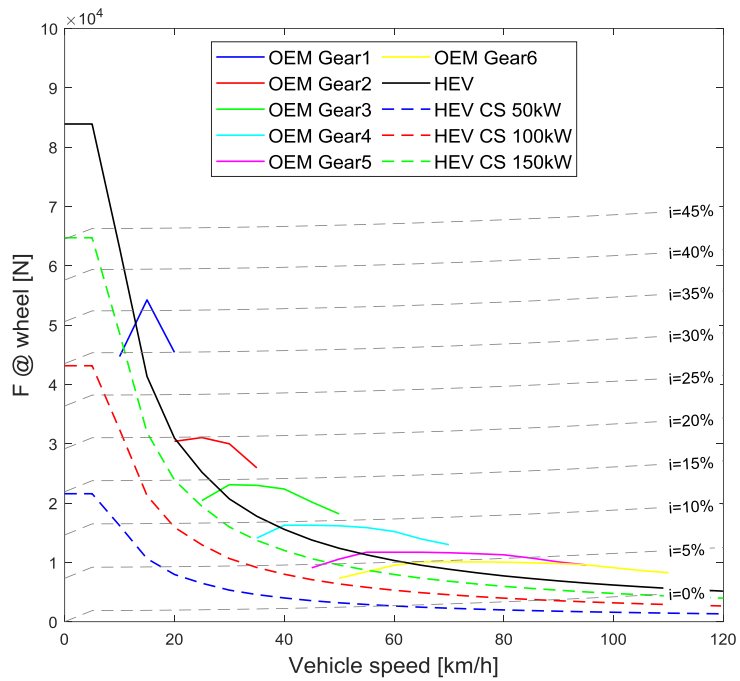
319

320

321

322

Figure 11 that is not common to find road grade higher than 20% and negligible cases more than 30%. Therefore, from a performance perspective the ICE need at least 100 kW to have an acceptable performance in extreme conditions.



323

324

325

326

327

Figure 10 – Performance Analysis for REV and conventional non-hybrid powertrain in terms of wheel force for different vehicle speed and road grades.

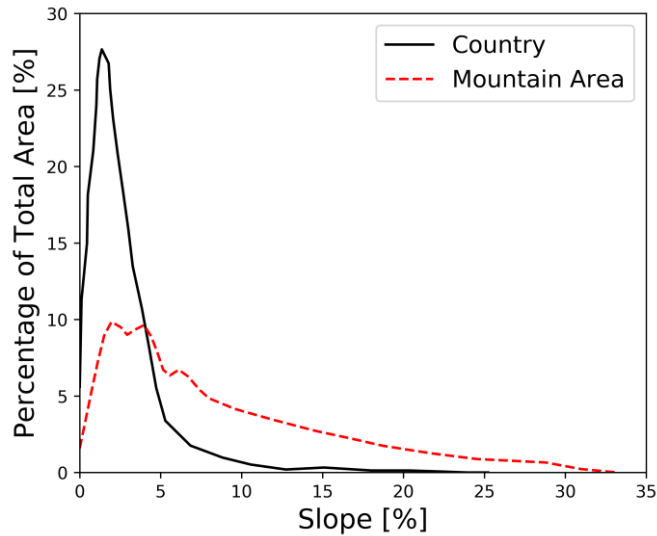


Figure 11 – Slope gradient analysis of urban expansion in China [36]. Representative of extreme normal and extreme condition that the buses can be used.

2.4. Combustion Concept

Having the right size of the battery package and ICE, now it is time to select the engine to apply the low temperature combustion mode. In this work, an Intelligent Charge Compression Ignition combustion mode in a 4-cylinder 5 L engine originally designed to operate under CDC was taken. Modification as additional DI and PFI for LRF is done. Main engine specification are shown in Table 2 and calibration strategy can be found in [24].

The main benefits of the ICCI with respect to RCCI are the possibility of direct injection of the LRF as well as the HRF. In RCCI the port injection with the fixed inlet angle might cause rich fuel areas and fuels being trapped in crevice regions, both of which would increase emissions of HC and CO emissions. In addition, the ICCI improves the LRF stratification in the combustion chamber due to the injection timing change during compression stroke. The ICE calibration at different rotational speeds and loads was performed with flexible stratifications to control the heat release by adjusting injection parameters such as injection timings, stages of split injection, and energy ratios of fuels, among others. High reactivity fuel and low reactivity fuel were directly injected with a pressure of 140 MPa and 30 MPa, respectively. The temperature of lubricating oil and coolant were maintained within $85\pm 2^{\circ}\text{C}$ and $80\pm 2^{\circ}\text{C}$ for all operation conditions.

Table 2. ICE main specifications.

Engine Parameters	Value
Bore [mm]	114
Stroke [mm]	130
Number of Cylinder [-]	4
Total Volume [L]	5.3
Compression ratio [-]	18:1
EGR loop	High-Pressure
Boost method	Mechanical Turbocompounding
Direct Injection [-]	Eight injectors for HRF and LRF
Number of holes for DI [-]	Six holes injector
Piston geometry [-]	Conventional re-entrant bowl
Port fuel Injection [-]	Four injectors for LRF

353 Conventional fuels (Diesel, Gasoline) and renewable energy fuels (Biodiesel,
 354 Methanol and Butanol) are tested in stationary conditions. Main fuel specification is
 355 shown in Table 3. Table 3. Fuels specifications. Biodiesel is regarded as a promising alternative
 356 due to its similar properties with diesel and good performance in CI engines. Methanol
 357 has a low carbon content and a high oxygen content, potential to reduce soot, CO and
 358 HC. Lastly, Butanol compared to methanol and ethanol, has a lower vapor pressure,
 359 better blending ability, and greater energy density when used in ICE. All of the previous
 360 mentioned renewable energy fuels have the capability to reduce the well to wheel
 361 (WTW) CO₂ emissions due to the ultra-low well to tank (WTT) CO₂ values.

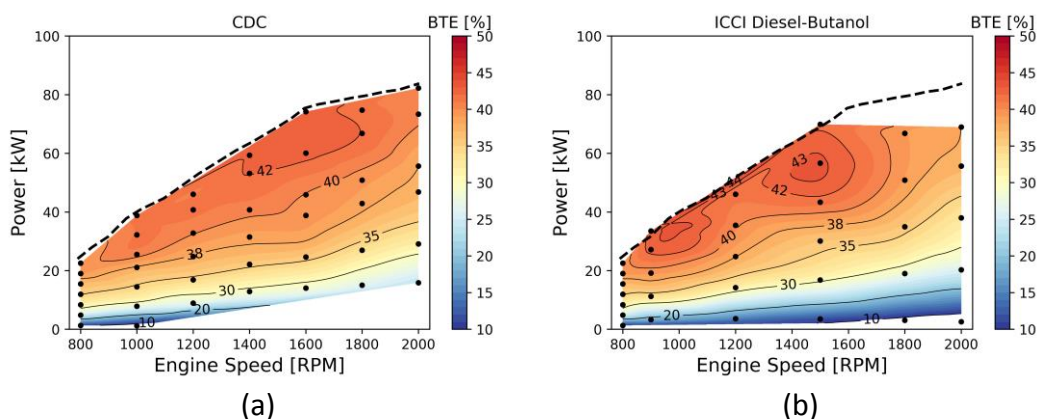
362

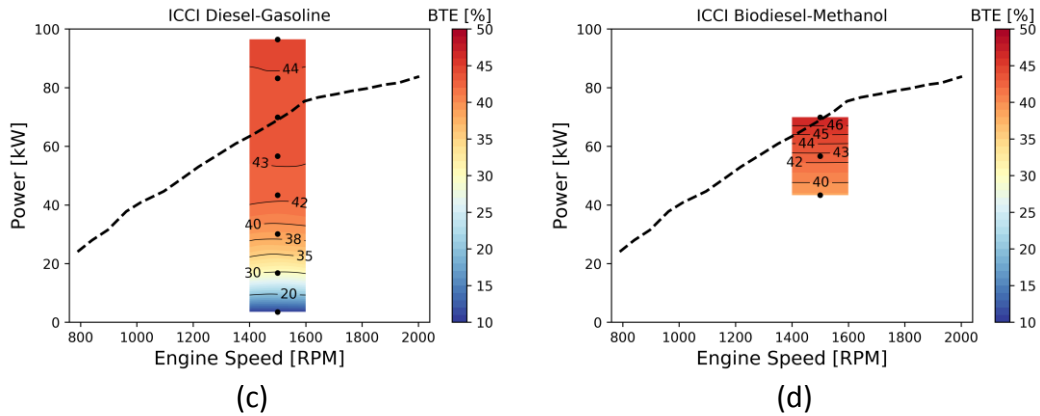
Table 3. Fuels specifications.

Fuel Parameters	Diesel	Gasoline	Biodiesel	Methanol	Butanol
Type of fuel [-]	HRF	LRF	HRF	LRF	LRF
Cetane Number [-]	53	-	53	5	25
Research Octane Number [-]	-	95	-	106	96
Lower heating Value [MJ/kg]	42.7	42.6	37.1	19.9	33.2
Flash Point [°C]	74	18	225	11	35
Density [g/L @20°C]	831	750	880	790	809
CO ₂ ratio [gCO ₂ /gfuel]	3.17	3.09	3.17	1.38	2.38
CO ₂ TTW [gCO ₂ /MJfuel]	74.2	72.5	85.4	69.3	69.2

363

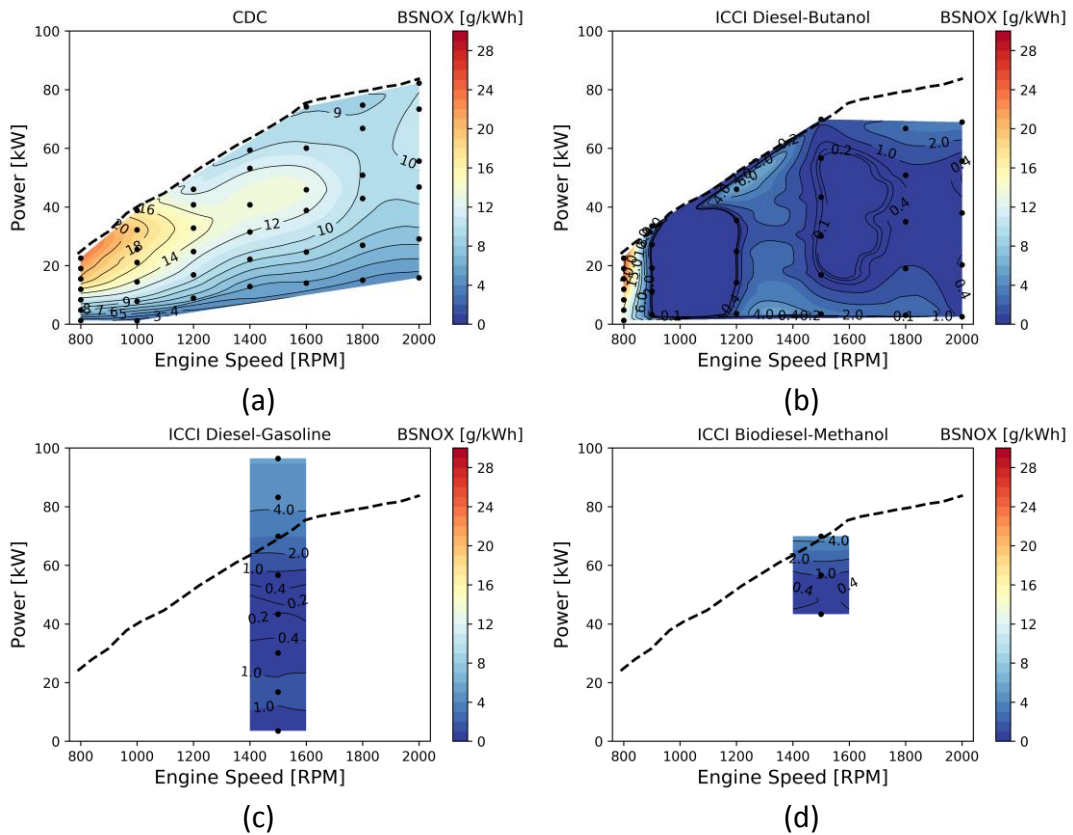
364 Figure 12 shows the brake thermal efficiency values for the calibrated points in
 365 CDC and ICCI mode. The original equipment manufacturer (OEM) diesel calibration
 366 achieves 42% of BTE at 60 kW and 1400 rpm. The ICCI Diesel-Butanol was calibrated
 367 in 26 operative conditions, with a maximum BTE of 43% at 55 kW and 1500 rpm. Due
 368 to the good performance of the ICE in this engine speed the other fuels in ICCI mode
 369 are calibrated in that region to reduce calibration cost. As the REV has an operation
 370 in particular engine points, it is not necessary an all calibration map. The ICCI with
 371 Diesel-Gasoline achieves 44% of BTE above 60 kW. In the case of Biodiesel-Methanol
 372 it was possible to achieve the highest BTE around 46%. The calibration setting as
 373 injection timing, fuel injected, EGR rate can be found in previous research group
 374 publications [22][23][24]. As change for each fuel, cannot be showed in the current
 375 manuscript for brevity reasons.





376 Figure 12 – Calibration map in terms of Brake Thermal Efficiency for different combustion modes.
 377 Conventional Diesel Combustion (a), ICCI Diesel Butanol (b), ICCI Diesel Gasoline (c) and ICCI Biodiesel
 378 Methanol (d). The experiments were performed in the ICE of Table 2.

379 The main advantage of ICCI is the possibility to reduce NO_x emissions due to the
 380 low combustion chamber temperature. The brake specific NO_x map is shown in
 381 Figure 13. It possible to note the high improvements with respect to the CDC, around
 382 one order of magnitude. In addition, the NO_x is below 0.4 g/kWh, current EUVI and
 383 China VI emissions limit. This means that it has potential to remove Selective
 384 Catalytic Reduction (SCR), Ammonia Slip Catalyst (ASC) and Urea injection. Diesel-
 385 Butanol under ICCI combustion shows the largest improvements in terms of NO_x
 386 followed by the Diesel-Gasoline.



387 Figure 13 – Calibration map in terms of Brake Specific NO_x engine-out emissions for different
 388 combustion modes. Conventional Diesel Combustion (a), ICCI Diesel Butanol (b), ICCI Diesel Gasoline (c)
 389 and ICCI Biodiesel Methanol (d). The experiments were performed in the ICE of Table 2.

390 **2.5. Life Cycle Analysis**

391 To have a global analysis of each powertrain potential an LCA is included considering
 392 Well to Tank, Tank to Wheel and vehicle fabrication, maintenance, and disposal CO₂
 393 generation. The CO₂ computation is done by a deep research bibliography in order to
 394 analyse component environmental impact in two scenarios (Europe and Asia) when is
 395 possible. The values taken for this study are depicted in Table 4. The reference source is
 396 added.

397 Table 4. CO₂ impact by fuel production, component production, maintenance and disposal.

Component	CO ₂ Europe	CO ₂ Asia
Diesel WTT [g _{CO2} /MJ _{Fuel}]	15.9 [31]	18.0 [37]
Gasoline WTT [g _{CO2} /MJ _{Fuel}]	13.1 [31]	16.5 [37]
Butanol WTT [g _{CO2} /MJ _{Fuel}]		-31.6 [38]
Methanol WTT [g _{CO2} /MJ _{Fuel}]		-42.0 [39]
Biodiesel WTT [g _{CO2} /MJ _{Fuel}]		-27.3 [40]
Electricity WTT [g _{CO2} /MJ _{Fuel}]	88 [41]	166 [32]
Battery Manufacturing [kg _{CO2} /kWh]	75 [42]	110 [42]
Conventional Powertrain [ton _{CO2} /Vehicle]		9.9 [43]
Hybrid Powertrain [ton _{CO2} / Vehicle]		16.7 [43]
Electric Powertrain [ton _{CO2} / Vehicle]		9.8 [43]
Bus body [ton _{CO2} / Vehicle]		45.1 [43]
Chassis [ton _{CO2} / Vehicle]		45.4 [43]
Conventional End of Life [ton _{CO2} /Vehicle]		12.2 [43]
Hybrid End of Life [ton _{CO2} / Vehicle]		11.9 [43]
Electric End of Life [ton _{CO2} / Vehicle]		13.7 [43]
Tires [kg _{CO2} /unit]		600 [44]
Water Cooling [g _{CO2} /lt]		1600 [45]
Oil Lubricant [g _{CO2} /lt]		2714 [45]
Transmission Lubricant [g _{CO2} /lt]		2140 [45]

398 The drop-in fuels (Diesel and Gasoline) are slightly higher in Asia than Europe due to
 399 higher transportation cost. China imported a little more than two thirds of its petroleum
 400 for domestic consumption and the percent of import will most definitely grow with time.
 401 About 90% of imported crude was shipped from overseas, primarily from the Middle
 402 East and Africa. The delivery of gasoline and diesel in China is primarily accomplished by
 403 rail and by ship along the coast and major rivers. Road delivery is used as supplements
 404 and for short-range distribution purposes. Pipeline delivery of gasoline and diesel
 405 remains rather limited presently.

406 On the other hand, the renewable energy fuels were taken the same values for both
 407 scenarios due to the uncertainties of the production conditions of these fuels. A range
 408 of minimum and maximum estimated in the bibliography are taken. The electricity mix
 409 is well tracked by several studies. As over 60% of total electricity in China is from coal
 410 firing and low renewable energy, it generates more GHG emissions than it does in the
 411 Europe. Electricity grid transmission and distribution losses are applied to each country
 412 based on International Energy Agency (IEA) statistics. On average at EU level
 413 transmission and distribution losses increase the carbon intensity of the grid by about
 414 7%. On top of this, 10% efficiency losses were added: 5% from the charger equipment
 415 and 5% from the battery charging efficiency. Therefore, the value of Table 5 is multiplied
 416 by 1.07 and then by 1.10 for each country.

417 Battery manufacturing is a crucial aspect in this work to a fair comparison between
 418 non-hybrid, REV and BEV. The research bibliography of [42] is taken as reference due to
 419 the deep analysis in different scenarios. In china the battery production will generate

420 more CO₂ emissions due to the energy mix. It is important to note that it is supposed
421 that the battery will be produced in Europe. If this scenario changes and the battery is
422 produced in China and send to Europe the trend will be revert. However, it was
423 preferred to supposed that the battery is produced in each continent.

424 The vehicle life was estimated in 16 years that is equivalent to 800,000 km. Vehicle
425 maintenance is separated into maintenance of the vehicle and tire replacement. It is
426 estimated 50 lt/year of oil lubricant, 150 lt/year refrigerant liquid and 13 lt/year
427 transmission lubricant. The tires are replaced each year (50,000 km) with six tires per
428 bus. The bus production and disposal are taken from [43] because analyse the vehicle
429 CO₂ impact for similar buses than are studied in the current work.

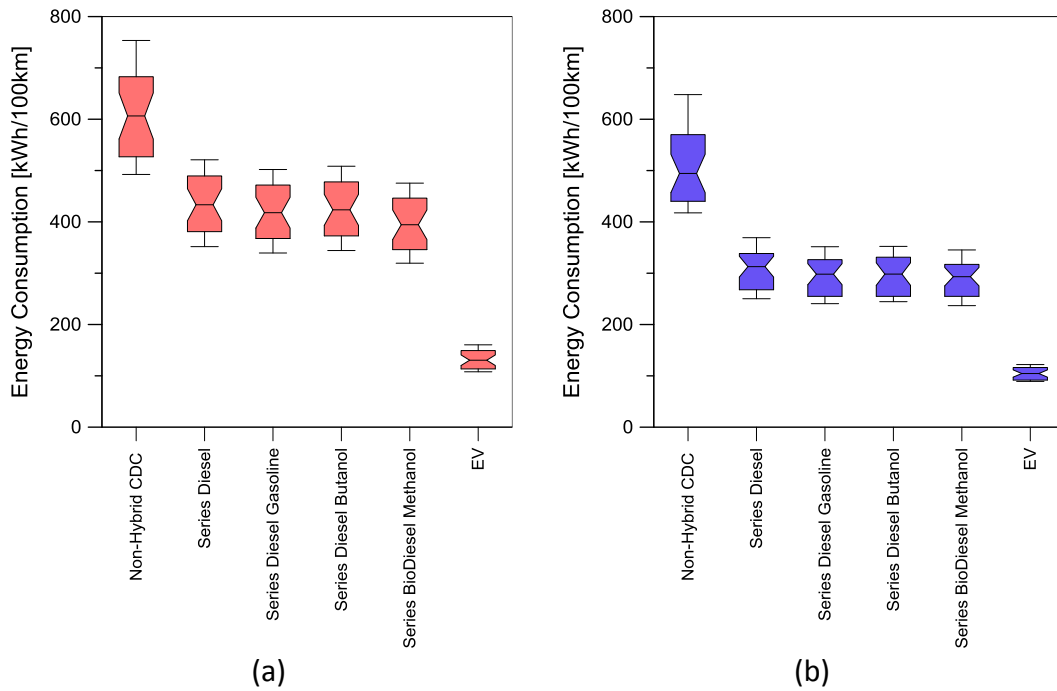
430 **3. Results**

431 **3.1. ICCI performance and emissions**

432 This section presents the performance and engine-out emissions of the ICCI REV bus
433 concept in Valencia and Shanghai driving cycles. The CDC non-hybrid and EV commercial
434 buses are included for comparison as well as the CDC REV. The model is based in map-
435 based approach where the power request to the engine and electric motors is calculated
436 in each instant based on the powertrain forces and the energy management strategy.
437 Therefore, the CDC and ICCI modes are changed by modify the engine map in the ICE
438 sub model. The calculus is based in the operation in steady state conditions. The
439 transient effect is considered negligible for this concept. This is in line with the results
440 showed by the authors in previous publications [13][46][47].

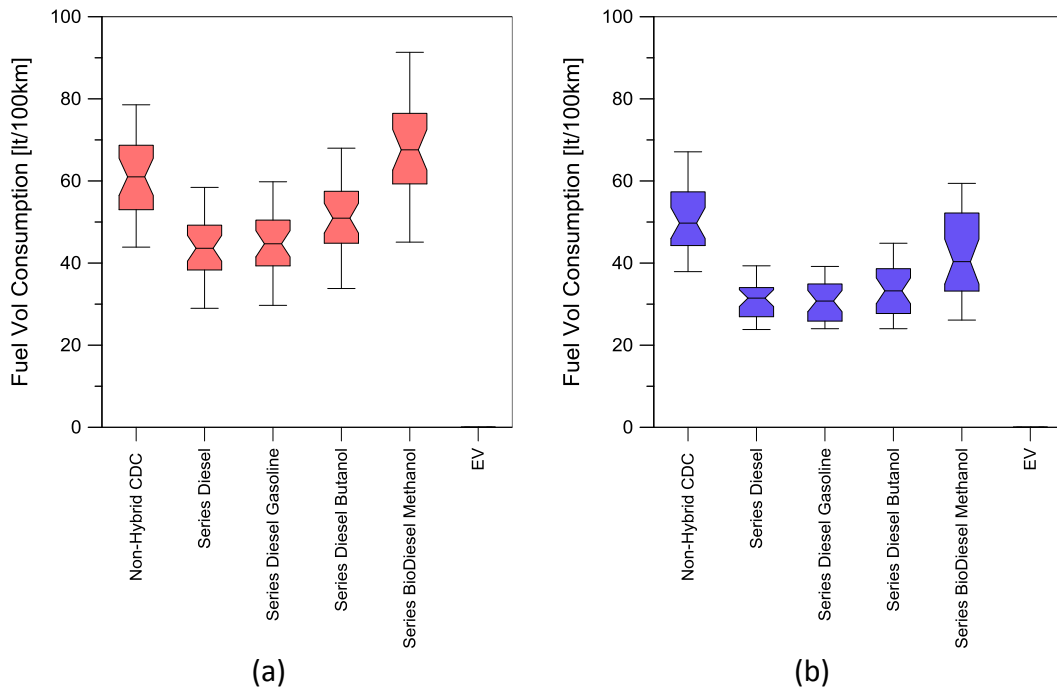
441 The following figures show a Notched box plot. This type of graph depicts the
442 median, minimum, maximum and confidence interval. For this case 10/90 percentile is
443 used. The data groups the results for each combustion concept and fuels in the case of
444 three passenger load (0, 35 and 70 passengers) and ten driving cycles. Figure 14 shows
445 the energy consumption for all vehicles. In both scenarios the EV is the most efficiently
446 followed by the REV. As the maximum BTE of all fuels combinations is similar, the ICCI in
447 the hybrid vehicle has similar energy reductions. The Biodiesel-methanol case shows
448 slightly improvements due to the 45% of BTE. The absence of the ICE makes the BEV
449 80% more efficiently than the non-hybrid. The hybrid was close to 30% of energy
450 reductions thanks to the higher ICE efficiently and regenerative braking. The avoid of
451 idle phase also allows to energy saving. For all cases Valencia cycles presents higher
452 energy consumption due to higher vehicle speed than in Shanghai.

453 The fuel volume consumption (see Figure 15) evidence the effect of lower heating
454 value of the renewable energy fuels. The worst case is the Biodiesel-Methanol due to
455 the 53% of lower LHV of methanol with respect to diesel (see Table 3). Secondly the
456 Diesel-Butanol due to the 20% lower LHV of butanol than diesel. However, for this case
457 the average fuel consumption is lower than the non-hybrid diesel. Both, Valencia and
458 Shanghai cycles presents similar trends with the REV pure diesel the best case between
459 the concepts that have liquid fuel consumption.



460 Figure 14 – Energy Consumption 0, 35 and 70 passengers in Valencia (a) and Shanghai (b).

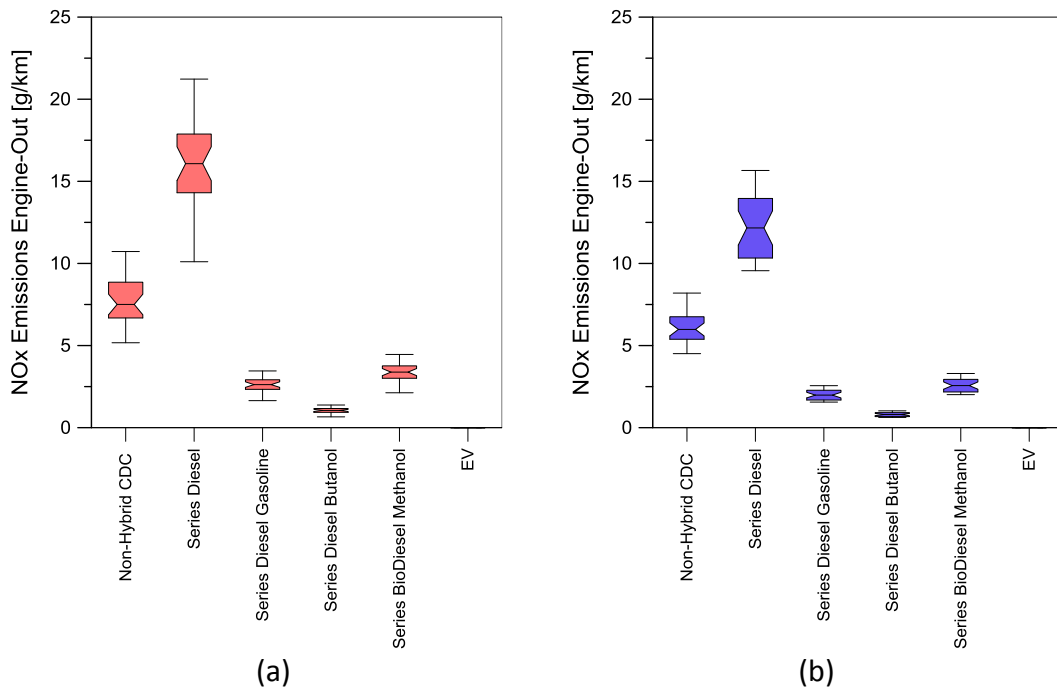
461



462 Figure 15 – Fuel Volume Consumption 0, 35 and 70 passengers in Valencia (a) and Shanghai (b).

463 Engine-out emissions are an important task to understand the possibility of LTC to
 464 achieve EUVI or China VI emissions without ATS. Also, it is possible to understand if it is
 465 possible to achieve ultra-low value thinking in current ATS for EUVII and China VII. Figure
 466 16 shows the improvements of the ICCI concept with different fuels in terms of NOx
 467 emissions. The use of a REV in diesel increase the NOx emissions. This is a disadvantage
 468 that will produce higher Urea consumption to mitigate the higher NOx emissions than
 469 the non-hybrid. The lowest value was achieved with Diesel-Butanol thanks to the 0.2

470 g/kWh obtained in the engine calibration process. The main advantage of the EV is the
 471 absence of tailpipe emissions.



472 Figure 16 – NOx Engine-out 0, 35 and 70 passengers in Valencia (a) and Shanghai (b).

473 The main disadvantage of ICCE concept is the higher CO and HC engine-out emissions.
 474 The indirect injection of the second fuel (Gasoline, Butanol or Methanol) make the
 475 trapped fuel in the crevices produces large pollutant emissions as was seen in
 476 commercial application for gasoline engines. Figure 17 shows the average values in
 477 Valencia driving cycles. Shanghai present similar trends and is avoid to include the graph
 478 for brevity of the manuscript. The values are one order of magnitude higher than Diesel
 479 operating in non-hybrid and REV mode. These values are important to obtain to future
 480 oxidation catalyst evaluations [46]. The CO emissions are higher than HC. However, EU
 481 VI is stricter in the last parameter. Therefore, HC emissions need to be studied in the
 482 future for this type of combustion concept. The Biodiesel-Methanol was the best dual
 483 fuel case with 7 g/km instead of 11.5 g/km of the Diesel-Gasoline.

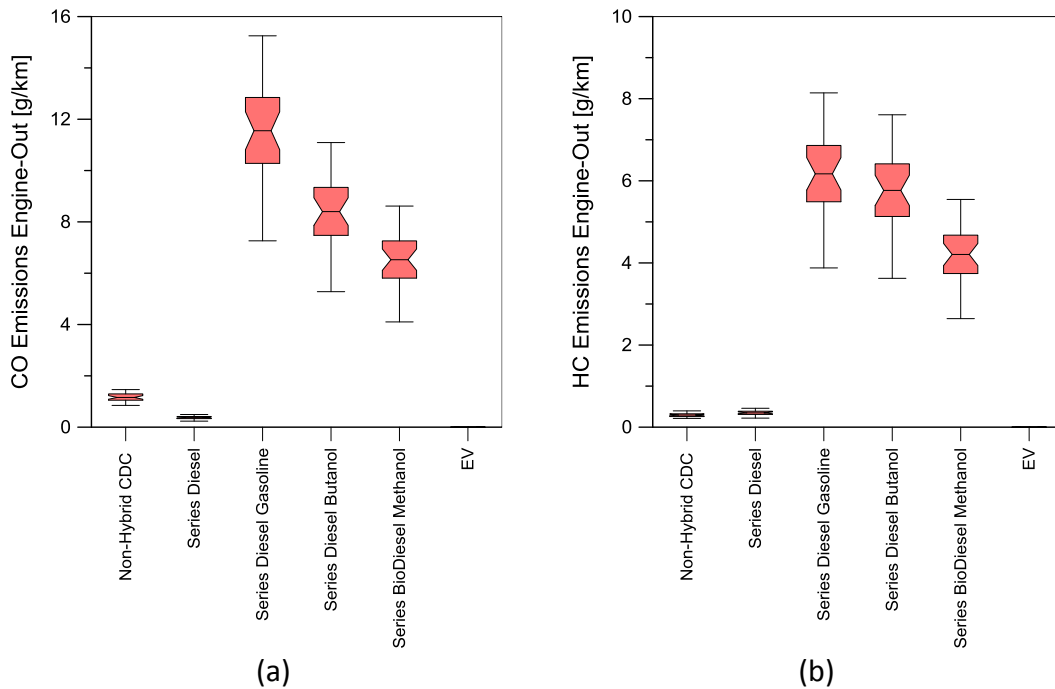


Figure 17 – Engine-out CO (a) and HC (b) 0, 35 and 70 passengers in Valencia.

484

485

3.2. Life Cycle Analysis

486

487

488

489

490

491

492

493

494

495

496

497

In terms of CO₂ emissions, a WTW and LCA analysis is done. Figure 18 shows the WTW after including the TTW CO₂ emissions calculated with vehicle model simulations and WTT CO₂ emissions from Table 4. The REV in drop-in fuels as Diesel and Gasoline shows around 30% of WTW emissions reduction with respect to CDC non-hybrid in Valencia and 40% in Shanghai. This is a large fuel saving if consider that only a series hybrid hybridization is applied. Using renewable energy fuels, the gains increase to 65% with Diesel-butanol and 75% with Biodiesel-Methanol in average for Valencia and Shanghai. The results for EV are comparable with the REV Biodiesel-Methanol thanks to the ultra-low WTT of the renewable energy fuels (see Table 4). The results for the EV bus are better for Valencia than Shanghai due to the high carbon content of the China electricity mix. In both cases the EV is also a good choice with improvements around 75% of WTW CO₂ emissions with respect to non-hybrid bus.

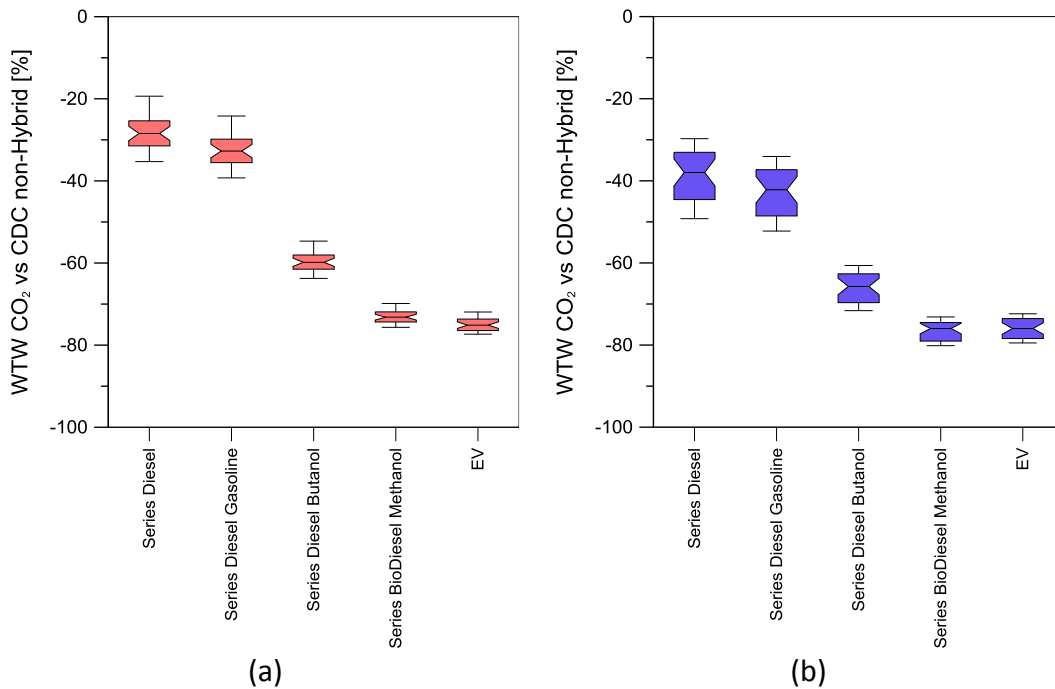


Figure 18 – WTW CO₂ emissions reduction percentage 0, 35 and 70 passengers in Valencia (a) and Shanghai (b) compared CDC non-hybrid.

498
499

500 When considering bus production, battery manufacturing, maintenance, and end of
 501 life the results have small variations seen in the LCA (see Figure 19). The main change is
 502 that the REV with two renewable energy fuels increase the CO₂ reduction with respect
 503 to the BEV case. This is due to the high CO₂ emissions during the battery production. The
 504 results are even improved in China scenario due to the higher carbon content of the
 505 electricity mix during battery production (see Table 4). A summary of the absolute values
 506 for 20 driving cycles (10 in Valencia and 10 in Shanghai) is presented in Figure 20. The
 507 baseline cases are showed in the spider graph Figure 20. It is possible to see an energy
 508 consumption of 117 kWh/100km instead of 560 kWh/100km of the non-hybrid. The REV
 509 was in 370 kWh/100km, 35% lower than the non-hybrid. The REV with renewable energy
 510 fuels shows similar energy consumption but low WTW and LCA CO₂ emissions. Other
 511 improvements are the smaller ICE than the non-hybrid and lower battery size than the
 512 pure BEV. The main disadvantage is the higher fuel volume consumption. For the large
 513 ICCI renewable energy fuel application it is necessary to produce the Butanol and
 514 Methanol at lower price than the Diesel or Gasoline.

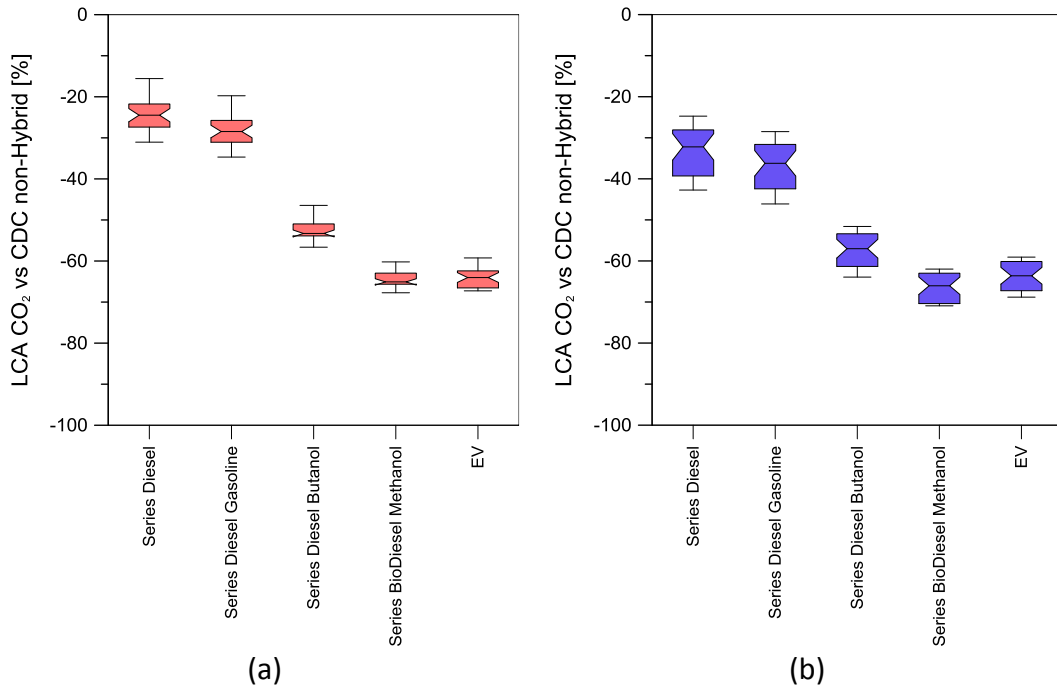


Figure 19 – LCA CO₂ emissions reduction percentage 0, 35 and 70 passengers in Valencia (a) and Shanghai (b) compared CDC non-hybrid.

515
516
517

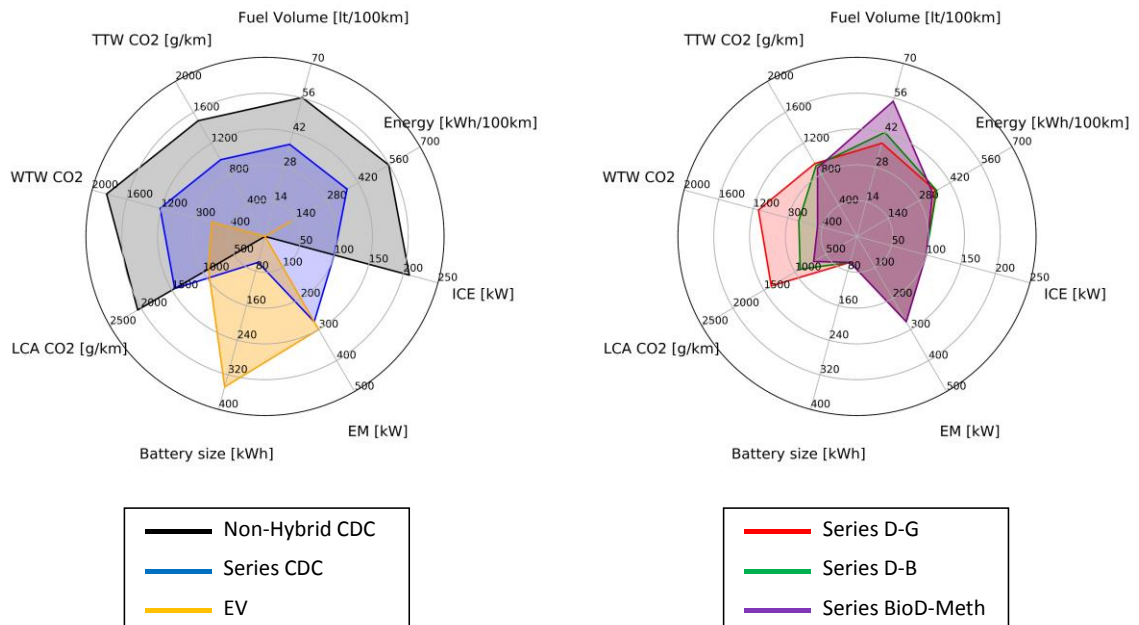


Figure 20 – LCA CO₂ emissions values average for 0, 35 and 70 passengers and Valencia, Shanghai cycles.

518
519
520
521

522 4. Conclusions

523 The manuscript presents novelty results in the area of renewable energy fuels
524 and electrification. The bus numerical models show the main advantages and drawbacks
525 of using a low temperature combustion concept in a series hybrid REV. The results are
526 presented against the most common commercial vehicles. Non-hybrid series and pure
527 electric bus are included. All cases are studied in two different scenarios: Europe and
528 Asia. The driving cycles were generated in Valencia and Shanghai. The LCA values are
529 taken from continent statistics from the bibliography.

530 The main findings of this work are:

- 531 • The REV allows 38% of energy saving with respect to the non-hybrid concept.
532 The most efficiently is the EV bus with 79% of energy reduction due to the
533 higher EM operation efficiency than the ICE even in dual fuel ICCI mode.
- 534 • The series hybrid operation allows to the REV in LTC to reduce 53% the engine-
535 out NOx emissions with Diesel-Gasoline with respect of the non-hybrid diesel.
536 The results are even better for Diesel-Butanol with 63% of reduction. This is
537 mainly due to the ultra-low NOx emissions at 1500 rpm and 60 kW in the
538 calibration process. The REV with CDC increase the NOx engine-out emissions
539 in 35% with respect to the same combustion concept in non-hybrid.
- 540 • The WTW and LCA are favourable for electrified powertrains with 30% for REV
541 without renewable fuels. The use of one renewable fuel (Diesel-Butanol) allows
542 to increase the LCA saving in 55%. The inclusion of a second biofuel (Biodiesel-
543 Methanol) allows 66% of LCA CO₂ reduction. These values are even higher than
544 the EV baseline that was 54% with respect to the non-hybrid.

545 Summarizing, the use of EV is a good way to reduce CO₂ impact. However, the
546 consideration of REV with biofuels is also a good solution for minimizing CO₂ impact in
547 the transportation sector. The ICCI combustion concept in this type of stationary
548 operation is ideal to also reduce engine-out emissions as NOx. Next steps in the
549 investigation will be to go a step forward in terms of concept application. Experimental
550 engine real driving cycles will be performed with the data obtained in the current
551 manuscript in terms of engine load and speed request. In addition, efforts will be applied
552 to understand the potential of current commercial oxidation catalyst to achieve Euro
553 legislation for the dual fuel concept.

554 Acknowledgments

555 Operación financiada por la Unión Europea a través del Programa Operativo del Fondo
556 Europeo de Desarrollo Regional (FEDER) de la Comunitat Valenciana 2014-2020 con el
557 objetivo de promover el desarrollo tecnológico, la innovación y una investigación de
558 calidad a través del Proyecto IDIFEDER/2020/34 "Equipamiento Para El Desarrollo De
559 Plantas Propulsivas Híbridas Limpias Y Eficientes A Través Del Uso De E-Fuels".

560 Abbreviations

ASC	Ammonia slip catalysts	HRF	High reactivity fuel
ATS	Aftertreatment systems	ICCI	Intelligent charge compression ignition
BEV	Battery electric vehicles	ICE	Internal Combustion Engine
BMEP	Brake mean effective pressure	LCA	Life cycle analysis
BSCO	Brake specific CO emissions	LHV	Low heating value
BSCO ₂	Brake specific CO ₂ emissions	LI-Ion	Litium Ion batteries
BSFC	Brake specific fuel consumption	LRF	Low reactivity fuel
BSHC	Brake specific HC emissions	LTC	Low temperature combustion
BSNO _x	Brake specific NO _x emissions	MBC	Manhattan bus cycle
BSSoot	Brake specific soot emissions	MHEV	Mild hybrid electric vehicle
BTE	Brake thermal efficiency	NO _x	Nitrogen Oxides
CDC	Conventional diesel combustion	OEM	Original equipment manufacturer
China VI	China six emission legislation for Heavy Duty vehicles	OMEx	Oxymethylene dimethyl ether Belt alternator starter hybrid powertrain
CI	Compression Ignition	P0	Parallel hybrid electric vehicle without clutch
CO	Carbon Monoxide	P1	Parallel hybrid electric vehicle pre transmission
CO ₂	Carbone dioxide	P2	Parallel hybrid electric vehicle pos transmission
CR	Compression ratio	P3	Premixed charge compression ignition
DI	Direct Injection	PCCI	Port fuel injection
DME	Dimethyl ether	PFI	Plug in electric vehicle
DOC	Diesel Oxidation Catalyst	PHEV	Reactivity Controlled Compression Ignition
DoE	Design of experiments	RCCI	Range extender vehicle
DPF	Diesel particle filter	REV	Selective catalytic reduction
EM	Electric machine	SCR	
EUVI	Euro six emission legislation for Heavy Duty vehicles	SI	Spark Ignition
FHEV	Full hybrid electric vehicle	SOC	State of the charge of the battery
GCI	Gasoline compression ignition	TM	Traction motor
Gen	Generation motor	TTW	Tank to wheel
HCCI	Homogeneous charge compression ignition	WTT	Well to tank
HEV	Hybrid electric vehicle	WTW	Well to wheel

561

562 5. References

- 563 [1] J. Dixon, W. Bukhsh, C. Edmunds, and K. Bell, "Scheduling electric vehicle
564 charging to minimise carbon emissions and wind curtailment," *Renew. Energy*,
565 vol. 161, pp. 1072–1091, 2020.
- 566 [2] S. Shojaabadi, S. Abapour, M. Abapour, and A. Nahavandi, "Simultaneous
567 planning of plug-in hybrid electric vehicle charging stations and wind power

- 568 generation in distribution networks considering uncertainties," *Renew. Energy*,
569 vol. 99, pp. 237–252, 2016.
- 570 [3] A. Lajunen, "Energy consumption and cost-benefit analysis of hybrid and electric
571 city buses," *Transp. Res. Part C Emerg. Technol.*, vol. 38, pp. 1–15, 2014.
- 572 [4] F. Millo, L. Rolando, R. Fuso, and J. Zhao, "Development of a new hybrid bus for
573 urban public transportation," *Appl. Energy*, vol. 157, pp. 583–594, 2015.
- 574 [5] M. Gerbec, R. O. Samuel, and D. Kontić, "Cost benefit analysis of three different
575 urban bus drive systems using real driving data," *Transp. Res. Part D Transp.
576 Environ.*, vol. 41, pp. 433–444, Dec. 2015.
- 577 [6] S. L. Hallmark, B. Wang, and R. Sperry, "Comparison of on-road emissions for
578 hybrid and regular transit buses," *J. Air & Waste Manag. Assoc.*, vol. 63, no. 10,
579 pp. 1212–1220, 2013.
- 580 [7] X. Hu, N. Murgovski, L. Johannesson, and B. Egardt, "Energy efficiency analysis of
581 a series plug-in hybrid electric bus with different energy management strategies
582 and battery sizes," *Appl. Energy*, vol. 111, pp. 1001–1009, 2013.
- 583 [8] J. Guo, Y. Ge, L. Hao, J. Tan, Z. Peng, and C. Zhang, "Comparison of real-world
584 fuel economy and emissions from parallel hybrid and conventional diesel buses
585 fitted with selective catalytic reduction systems," *Appl. Energy*, vol. 159, pp.
586 433–441, 2015.
- 587 [9] S. Zhang *et al.*, "Real-world fuel consumption and CO₂ emissions of urban public
588 buses in Beijing," *Appl. Energy*, vol. 113, pp. 1645–1655, 2014.
- 589 [10] D. M. Kim, P. Benoliel, D. K. Kim, T. H. Lee, J. W. Park, and J. P. Hong,
590 "Framework development of series hybrid powertrain design for heavy-duty
591 vehicle considering driving conditions," *IEEE Trans. Veh. Technol.*, vol. 68, no. 7,
592 pp. 6468–6480, 2019.
- 593 [11] E. Tazelaar, Y. Shen, P. A. Veenhuizen, T. Hofman, and V. D. B. P. P. J., "Sizing
594 Stack and Battery of a Fuel Cell Hybrid Electronic Intelligence in Vehicles
595 Distribution Truck," *Oil & Gas Sci. Technol.*, vol. 67, no. 4, 2012.
- 596 [12] L. Jiang *et al.*, "Hybrid charging strategy with adaptive current control of lithium-
597 ion battery for electric vehicles," *Renew. Energy*, vol. 160, pp. 1385–1395, 2020.
- 598 [13] A. García, J. Monsalve-serrano, R. L. Sari, and S. Martinez-boggio, "Energy
599 sustainability in the transport sector using synthetic fuels in series hybrid trucks
600 with RCCI dual-fuel engine," *Fuel*, vol. 308, no. July 2021, p. 122024, 2022.
- 601 [14] T. Zhao, Q. Ahmed, and G. Rizzoni, "Influence of battery charging current limit
602 on the design of range extender hybrid electric trucks," *2018 IEEE Veh. Power
603 Propuls. Conf. VPPC 2018 - Proc.*, 2019.
- 604 [15] V. Soloiu *et al.*, "Reactivity controlled compression ignition and low temperature
605 combustion of Fischer-Tropsch Fuel Blended with n-butanol," *Renew. Energy*,
606 vol. 134, pp. 1173–1189, 2019.
- 607 [16] P. Piqueras, A. García, J. Monsalve-Serrano, and M. J. Ruiz, "Performance of a

- 608 diesel oxidation catalyst under diesel-gasoline reactivity controlled compression
609 ignition combustion conditions,” *Energy Convers. Manag.*, vol. 196, no. June, pp.
610 18–31, 2019.
- 611 [17] ACEA, “ACEA Position Paper Views on proposals for Euro 7 emission standard,”
612 no. December, p. 18, 2020.
- 613 [18] A. P. Ragon and F. Rodríguez, “Estimated cost of diesel emissions control
614 technology to meet future Euro VII standards,” no. April, pp. 1–27, 2021.
- 615 [19] B. J. Lawler and Z. S. Filipi, “Integration of a Dual-Mode SI-HCCI Engine Into
616 Various Vehicle Architectures,” *J. Eng. Gas Turbines Power*, vol. 135, no. 5, p.
617 052802, 2013.
- 618 [20] S. L. Kokjohn, R. M. Hanson, D. A. Splitter, and R. D. Reitz, “Experiments and
619 Modeling of Dual-Fuel HCCI and PCCI Combustion Using In-Cylinder Fuel
620 Blending,” *SAE Int. J. Engines*, vol. 2, no. 2, pp. 2009-01–2647, Nov. 2009.
- 621 [21] J. Benajes, A. García, J. Monsalve-Serrano, and S. Martínez-Boggio, “Emissions
622 reduction from passenger cars with RCCI plug-in hybrid electric vehicle
623 technology,” *Appl. Therm. Eng.*, vol. 164, no. September 2019, p. 114430, Jan.
624 2020.
- 625 [22] Z. L. Li, Y. Qian, G. Huang, W. Bin Zhao, Y. Y. Zhang, and X. C. Lu, “Gasoline-diesel
626 dual fuel intelligent charge compression ignition (ICCI) combustion: Conceptual
627 model and comparison with other advanced combustion modes,” *Sci. China
628 Technol. Sci.*, vol. 81, no. Icci, 2020.
- 629 [23] G. Huang *et al.*, “Effects of fuel injection strategies on combustion and emissions
630 of intelligent charge compression ignition (ICCI) mode fueled with methanol and
631 biodiesel,” *Fuel*, vol. 274, no. February, p. 117851, 2020.
- 632 [24] Z. Li *et al.*, “Control of intake boundary conditions for enabling clean combustion
633 in variable engine conditions under intelligent charge compression ignition (ICCI)
634 mode,” *Appl. Energy*, vol. 274, no. January, p. 115297, Sep. 2020.
- 635 [25] Man, “MAN LION’S CITY 12,” p. 775.
- 636 [26] “BYD-eBus-Elektrobus-12-M-GSK-Lifepocenter-Nord.” .
- 637 [27] IVECO BUS, “Iveco Urbanway Euro Vi,” no. 286 Cv, 2014.
- 638 [28] A. García, J. Monsalve-Serrano, S. Martinez-Boggio, P. Gaillard, O. Poussin, and
639 A. A. Amer, “Dual fuel combustion and hybrid electric powertrains as potential
640 solution to achieve 2025 emissions targets in medium duty trucks sector,”
641 *Energy Convers. Manag.*, vol. 224, no. June, p. 113320, Nov. 2020.
- 642 [29] R. Du, X. Hu, S. Xie, L. Hu, Z. Zhang, and X. Lin, “Battery aging- and temperature-
643 aware predictive energy management for hybrid electric vehicles,” *J. Power
644 Sources*, vol. 473, no. June, p. 228568, 2020.
- 645 [30] JSOL-Corporation, “Motor design tool Jmag international,” 2020. [Online].
646 Available: <https://www.jmag-international.com/express/>. [Accessed: 26-May-
647 2020].

- 648 [31] R. Edwards *et al.*, *WELL-TO-TANK (WTT) Report. Appendix 1 - Version 4a -*
649 *Conversion factors and fuel properties WELL-TO-WHEELS*. 2013.
- 650 [32] X. Li, K. J. Chalvatzis, and D. Pappas, "China's electricity emission intensity in
651 2020 - An analysis at provincial level," *Energy Procedia*, vol. 142, no. January
652 2018, pp. 2779–2785, 2017.
- 653 [33] Mapbox, "Mapbox." [Online]. Available: <https://www.mapbox.com/>.
- 654 [34] M. Sivak, "ASSUMED VERSUS ACTUAL WEIGHTS OF VEHICLE PASSENGERS," no.
655 January, 2017.
- 656 [35] Ornl, "Manhatan Bus cycle." [Online]. Available:
657 <https://www.nrel.gov/transportation/drive-cycle-tool/>.
- 658 [36] L. Zhou, X. Dang, H. Mu, B. Wang, and S. Wang, "Cities are going uphill: Slope
659 gradient analysis of urban expansion and its driving factors in China," *Sci. Total*
660 *Environ.*, vol. 775, p. 145836, 2021.
- 661 [37] W. Shen, W. Han, D. Chock, Q. Chai, and A. Zhang, "Well-to-wheels life-cycle
662 analysis of alternative fuels and vehicle technologies in China," *Energy Policy*,
663 vol. 49, no. October, pp. 296–307, 2012.
- 664 [38] A. Nilsson, K. Shabestary, M. Brandão, and E. P. Hudson, "Environmental
665 impacts and limitations of third-generation biobutanol: Life cycle assessment of
666 n-butanol produced by genetically engineered cyanobacteria," *J. Ind. Ecol.*, vol.
667 24, no. 1, pp. 205–216, 2020.
- 668 [39] G. Zang, P. Sun, A. Elgowainy, and M. Wang, "Technoeconomic and Life Cycle
669 Analysis of Synthetic Methanol Production from Hydrogen and Industrial
670 Byproduct CO₂," *Environ. Sci. Technol.*, 2021.
- 671 [40] W. Gerbens-Leenes and K. Holtz, "Consequences of transport low-carbon
672 transitions and the carbon, land and water footprints of different fuel options in
673 the Netherlands," *Water (Switzerland)*, vol. 12, no. 7, 2020.
- 674 [41] European Environment Agency, "CO₂ emission intensity," 2021. [Online].
675 Available: [https://www.eea.europa.eu/data-and-maps/daviz/co2-emission-intensity-5#tab-googlechartid_chart_11_filters=%7B%22rowFilters%22%3A%7B%7D%3B%22columnFilters%22%3A%7B%22pre_config_ugeo%22%3A%5B%22European Union \(current composition\)%22%5D%7D%7D](https://www.eea.europa.eu/data-and-maps/daviz/co2-emission-intensity-5#tab-googlechartid_chart_11_filters=%7B%22rowFilters%22%3A%7B%7D%3B%22columnFilters%22%3A%7B%22pre_config_ugeo%22%3A%5B%22European Union (current composition)%22%5D%7D%7D). [Accessed: 24-May-2021].
- 680 [42] Transport & Environment, "How clean are electric cars?," pp. 1–33, 2020.
- 681 [43] A. Nordelöf, M. Romare, and J. Tivander, "Life cycle assessment of city buses
682 powered by electricity, hydrogenated vegetable oil or diesel," *Transp. Res. Part*
683 *D Transp. Environ.*, vol. 75, no. September, pp. 211–222, 2019.
- 684 [44] Y. Dong, Y. Zhao, M. U. Hossain, Y. He, and P. Liu, "Life cycle assessment of
685 vehicle tires: A systematic review," *Clean. Environ. Syst.*, vol. 2, no. March, p.
686 100033, 2021.
- 687 [45] A. N. Laboratory, "GREET® Model," 2021. [Online]. Available:

- 688 <https://greet.es.anl.gov/>. [Accessed: 24-May-2021].
- 689 [46] A. García, J. Monsalve-Serrano, R. Lago Sari, and S. Martinez-Boggio, "Energy
690 assessment of an electrically heated catalyst in a hybrid RCCI truck," *Energy*, vol.
691 238, p. 121681, 2022.
- 692 [47] A. García, P. Carlucci, J. Monsalve-Serrano, A. Valletta, and S. Martínez-Boggio,
693 "Energy management optimization for a power-split hybrid in a dual-mode RCCI-
694 CDC engine," *Appl. Energy*, vol. 302, no. June, p. 117525, 2021.
- 695